Original Article

http://dx.doi.org/10.3348/kjr.2011.12.6.686
pISSN 1229-6929 · eISSN 2005-8330
Korean J Radiol 2011;12(6):686-692

Korean Journal of Radiology
KJR

Isolated Noncompaction of Ventricular Myocardium: a Magnetic Resonance Imaging Study of 11 Patients

Hong Yun, PhD, Meng-su Zeng, MD, PhD, Hang Jin, MD, Shan Yang, MD

All authors: Department of Radiology, Zhongshan Hospital, Fudan University and Shanghai Medical Imaging Institute, 200032 Shanghai, China

Objective: To retrospectively summarize the cardiac magnetic resonance imaging (CMRI) findings of isolated noncompaction of ventricular myocardium (INVM).

Materials and Methods: Eleven patients (M:F = 9:2; mean age, 35 years) were evaluated. Steady-state free precession (SSFP), fast spin echo (SE) sequence, SSFP cine imaging, and delayed enhanced inversion recovery spoiled gradient echo (IR-SPGR) sequence were used for showing abnormal myocardium, measuring ratio of noncompacted/compacted myocardium layers (NC/C ratio), and detecting myocardial viability. The left ventricle was divided into nine segments and a NC/C ratio > 2.3 in diastole was used as cutoff value in diagnosing left INVM. The right ventricle was assessed qualitatively.

Results: Cardiac MRI indicated left INVM in seven patients, right INVM in one patient and biventricle INVM in three patients. Characteristic CMRI changes included prominent trabeculations, deep intertrabecular recesses and an increase in the NC/C ratio. The most frequently involved segments was left ventricular apex. Three patients had abnormal high signals within the trabecular structures on SE T2 weighted image. One ventricular aneurysm and one apical thrombus were also observed. Delayed enhancement was seen in six of nine patients with subendocardial and transmural patterns.

Conclusion: There are CMRI features that might be characteristic for INVM.

Index terms: *Isolated noncompaction of ventricular myocardium; Cardiac magnetic resonance imaging; Cardiomyopathy*

INTRODUCTION

As a new clinical and pathological group, noncompaction of the ventricular myocardium (NVM) is categorized as primary cardiomyopathy by the American Heart Association (AHA) (1). It was first described in 1990 and is thought to be related to the arrest of myocardial development (2). It is characterized by prominent trabeculations on the luminal surface of the ventricle, deep intertrabecular recesses communicating with ventricular lumen and regional wall motion abnormalities. Though it usually affects the left ventricle (LV) alone, right ventricular (RV) noncompaction may also be involved (< 50% of cases) (3). NVM can be isolated (without other structural cardiac abnormalities) and or co-exist with other congenital cardiac malformations. This cardiac abnormality is increasingly detected by echocardiography, computed tomography (CT) and magnetic resonance imaging (MRI). However, there is no universally accepted definition and diagnostic criteria of NVM and many cases are easily overlooked or misdiagnosed in clinical practice. CMRI is an excellent modality for the noninvasive assessment of patients with NVM, for its high resolution, multiplane imaging and superior contrast between the myocardium and intracardiac blood-pool (3-5). Currently, there are few studies describing the MRI features of NVM. The purpose of our study was to summarize and

Received April 12, 2011; accepted after revision June 30, 2011.
Corresponding author: Meng-su Zeng, MD, PhD, Department of Radiology, Zhongshan Hospital, Fudan University and Shanghai Medical Imaging Institute, 180#, Feng Lin Road, 200032 Shanghai, China.
• Tel: (861381) 737-3641 • Fax: (8261) 6443-9906
• E-mail: zeng-mengsu@zs-hospital.sh.cn

Korean Journal of Radiology
KJR

describe abnormal changes in CMRI in patients with isolated noncompaction of ventricular myocardium (INVM).

MATERIALS AND METHODS

Patient Population

Eleven patients were enrolled between January 2009 to April 2010. They were at first suspected cases of INVM by echocardiography, but then recommended to undergo CMRI and diagnosed with INVM by CMRI. Exclusion criteria for performing CMRI included general contradictions to MRI examination (claustrophobia, pacemaker, coronary stents, bypass grafts and aneurysm clamp). Detailed information about history of drug allergies and renal function were acquired before contrast administration. Our institution does not require Institutional Review Board (IRB) approval for this retrospective study and informed consent was waived.

Clinical Data

The clinical features of 11 patients were recorded by cardiologists when they first presented to the hospital. Electrocardiographic (ECG) findings were evaluated by two cardiologists (with more than 5 years and 10 years experience with ECG diagnosis, respectively). The clinical data of 11 patients were acquired by electronic medical record systems and then comprehensively reevaluated by a senior cardiologist.

Cardiac MRI

Cardiac MRI was performed on a 1.5-Tesla (T) clinical scanner (Magnetom Avanto; Siemens AG, Erlangen, Germany) equipped with quantum gradients (slope, 45 mT/m; slew rate, 200 mT/m/s) and a six-element coil for each patient. Three ECG leads were placed on the left anterior hemithorax (vector ECG) and readjusted to obtain reasonable amplitude and a clean signal trace in the monitoring display.

The MRI sequences and parameters were as follows: Axial steady-state free precession (SSFP) (repetition time [TR]/ echo time [TE], 292.1/1.22 ms; matrix, 136 x 256; spatial resolution, 2.0 x 1.3 x 6.0 mm) and a coronal single shot fast spin echo sequence (SS-FSE) (TR/TE, 959.0/26.0 ms; matrix, 104 x 256; spatial resolution, 2.3 x 1.3 x 6.0 mm) were initially obtained covering the whole heart. All the localization sections including the 2-chamber, 4-chamber, and short-axis sections were acquired using SSFP with the following parameters: TR/TE, 300/1.21 ms; spatial resolution, 2.1 x 1.3 x 8.0 mm. Dark-blood fast spin echo (SE) T1-weighted sequence (TR/TE, 842.1/30 ms; matrix, 125 x 256; spatial resolution, 2.2 x 1.3 x 5.0 mm) and fast SE T2-weighted sequence (TR/TE, 1725.5/77 ms; matrix, 160 x 256; spatial resolution, 1.7 x 1.3 x 5.0 mm) were subsequently performed in LV short-axis and long-axis views. All SE images were acquired in end-diastole and SSFP cine imaging (TR/TE, 39.75/1.12 ms; matrix, 156 x 192; spatial resolution, 1.8 x 1.8 x 6.0 mm) with GRAPPA (generalized autocalibrating partially parallel acquisition) paralleling imaging at an acceleration factor of two were carried out in a 2-, 4-chamber and LV short-axis covering whole LV. T-SENSE parallel imaging was alternatively used for the patients with poor breath-hold behavior using an acceleration factor of three to speed up the acquisition. In nine patients, 0.2 mmol/kg body weight of Gadopentetate Dimeglumine (Magnevist; Schering AG, Berlin, Germany) was injected using a power injector at a rate of 2 ml/s, followed immediately by 20 ml of saline at the same rate. Ten to fifteen minutes after contrast administration, delayed-enhancement MRI was performed using the inversion recovery spoiled gradient echo (IR-SPGR) (TR/TE, 670/3.36 ms; matrix, 156 x 256; spatial resolution, 2.0 x 1.5 x 8.0 mm; time to inversion, 200-350 ms) with magnitude and phase sensitive reconstruction in ventricular long-axis and short-axis views.

Cardiac MRI Diagnostic Criteria

Diagnostic criteria of left INVM typically included the presence of prominent or numerous trabeculations, multiple deep intertrabecular recesses communicating with the ventricular cavity, and a two-layered appearance of the myocardium with an increased ratio of noncompacted to compacted myocardium (NC/C ratio > 2.3) in diastole (4).

The RV apex often presents with hypertrophic trabeculae in a normal individual, so it is difficult to differentiate between variants of normal and pathologic patterns. In previous studies, no specific CMRI criteria have been proposed for the diagnosis of right INVM due to the small sample size described. In this study, echocardiographic criteria for right INVM, including prominent two-layered structure, deep intertrabecular spaces communicating with RV cavity and thickness of the noncompacted RV greater than 75%, were used (6).

Cardiac MRI Data Analysis

All images were evaluated by two senior radiologists (more than 10 years experience with cardiovascular imaging),

and disagreement of evaluation was settled by a consensus reading.

Cine images were analyzed with the Argus software (Siemens). The LV wall was divided into nine segments: the whole apex was one segment (apical segment); at the base and at the midventricular level, the LV was divided into four segments each (inferior, lateral, anterior and septal) (3). In LV, the ratio of NC/C was measured manually on the long-axis and short-axis view on the SSFP cine sequence in diastole. At the base and mid-ventricular level for the short-axis view, the location with the most pronounced trabeculations were chosen for measurement of the thickness of noncompacted and the compacted myocardium perpendicular to the compacted myocardium. The NC/C ratio of each segment was independently measured by two readers and their mean value was used for the final diagnosis. The apex was measured on long-axis of LV using the same method. Ventricular volume was measured as normal or dilated.

Delayed-enhancement segments were independently judged visually on magnitude and phase sensitive reconstruction images in ventricular long-axis and short-axis views by two readers, and disagreement was settled by a consensus reading.

RESULTS

Clinical Data

The patient series consisted of 11 patients; nine males and two females with a mean age of 35 years and an age range of 15-58 years old. Eight patients (8 of 11, 73%) were referred to our hospital with a history of chest tightness or palpitations. One (1 of 11, 9%) suffered from sudden syncope and one adolescent patient (1 of 11, 9%) from sudden edema in extremities. One (1 of 11, 9%) was asymptomatic and detected by echocardiographic examination by chance.

Electrocardiographic findings were summarized as followed: three patients (3 of 11, 27%) with normal ECG performance, one (1 of 11, 9%) with LV high voltage, one (1 of 11, 9%) with RV high voltage, left atrium hypertrophy and ST-T changes, one (1 of 11, 9%) with only ST-T changes, two (2 of 11, 18%) with pre-excitation syndrome, and three (3 of 11, 27%) with ventricular premature contraction. The patient clinical data were summarized in Table 1.

Cardiac MRI Data

Right INVM (1 of 11, 9%), left INVM (7 of 11, 64%), and bilateral INVM (3 of 11, 27%) were found. In SSFP combined with fast SE sequence, prominent ventricular trabeculations, deep intertrabecular recesses communicating with ventricle cavity, and a regional ventricular motion abnormality were found. Fast SE sequence showed myocardial wall structure with both a thin epicardial compacted zone and an extremely thickened endocardial noncompacted zone which mimicked hypertrophic cardiomyopathy (Fig. 1). Three patients showed high signals within the trabecular structures on black-blood fast SE T2-weighted sequence, providing obvious contrast with black blood in the cavity. The SSFP cine sequence displayed a two-layered structure of ventricular myocardium consisting of an outer thinning layer and inner spongiform layer. It also showed high signals within the trabecular recesses suggestive of blood flow communicating with the ventricular cavity (Fig. 2).

A total of 99 segments were analyzed in the LV and noncompacted segment was found in 36 segments (36 of 99, 36%). The left apex was the most frequently affected segment (10 of 99, 10%), in ten of eleven patients (10 of 11, 91%); seven mid-lateral, six mid-anterior, six mid-inferior, three basal-anterior and three basal-lateral segments were also found to be affected. The basal-inferior was the least affected segment with only one segment was involved. In this study, there was no basal-septal or mid-septal segment affected. The mean NC/C ratio of the 36 segments was 3.1, with a range of 2.3-9.2, and a maximum NC/C ratio happened on the apex.

Systolic function of the LV wall was impaired to some degree in nine patients and normal cardiac function was only measured in two patients (No. 1 and No. 10). The average LV ejection fraction in the 11 patients was 40% (range: 23% to 70%), the LV end-diastolic volume and LV end-systolic volume were expanded to a different degree.

Delayed contrast-enhancement was performed in nine patients, with six patients having positive results (6 of 9, 67%). Only one case of apical delayed enhancement was found. The delayed enhancement area was present in both compacted and noncompacted segments and the patterns of enhancement included subendocardial and transmural myocardial enhancement.

Eight patients had dilated ventricles (8 of 11, 73%). Among the 10 patients with left involved NVM (7 with left NVM and 3 with bilateral NVM), seven had a dilated LV (7 of 10, 70%). Among the four patients with right involved NVM

Korean Journal of Radiology
KJR

Table 1. Patient Clinical Characteristics and Cardiac MR Imaging Findings

Patient	Gender	Age (Years)	Chief Complaint	ECG Changes	Noncompacted Segments	Delayed Enhancement	Other Findings
1	F	29	No complaint	Normal	RV-A	Normal	No other finding
2	M	45	Chest distress	Ventricular premature beat	LV-A, ML	Not perform	Dilated LV
3	M	36	Chest distress	Pre-excitation syndrome	LV-A, MA, ML, MI, BA, BL	Not perform	Dilated LV
4	M	56	Palpitation	Ventricular premature beat, intraventricular conduction blockage	LV-A, MA, ML, MI; RV	LV-MA, MS, MI, ML, BI, BS, RV	Dilated LV
5	M	34	Chest distress	LV high voltage	LV-A	LV-BL, ML, MI	LV hypertrophy
6	M	42	Palpitation	Normal	LV-A, MA, ML, MI	LV-MA, ML, MI, MS, BS	Abnormal signal and motion in interventricular septum
7	M	16	Edema in both lower extremities and right upper limb	RV high voltage, ST-T changes, left atrium hypertrophy	LV-A, RV	All segments of LV and RV	Entire heart dilated, mitral and tricuspid regurgitation, apical thrombus pericaridial effusion and pleural effusion
8	M	15	Chest distress	Pre-excitation syndrome, intraventricular conduction blockage	LV-A, MA, ML, MI	LV-MI, ML, MA, BL, BI	Entire heart dilated, mitral regurgitation, pericardial effusion
9	F	35	Palpitation	Ventricular premature beat	LV-A, BL, BA, MA, MI, ML	Normal	Dilated LV, ventricular aneurysm in LV apex
10	M	58	Chest distress	Normal	LV-A	Normal	Entire heart dilated
11	M	20	Sudden syncope	ST-T change	LV-A, BL, BA, BI, MA, MI, ML; RV	RV, LV-BI	RV and right atrium dilated

Note.— A = apex, BA = basal-anterior, BI = basal-inferior, BL = basal-lateral, LV = left ventricle, MI = midventricular-inferior, ML = midventricular-lateral, MS = midventricular-superior, RV = right ventricle

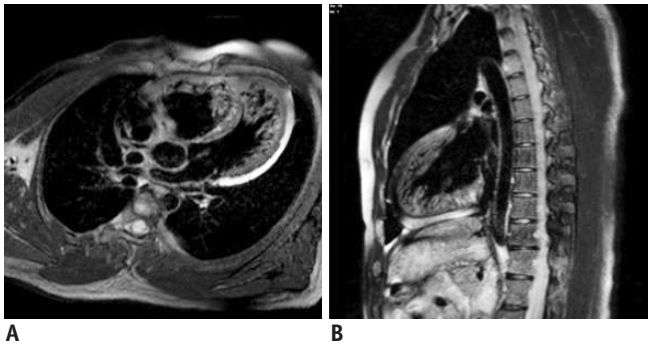

A B

Fig. 1. Spin echo sequence showing thin epicardial compacted zone and extremely thickened endocardial noncompacted zone in patient with biventricular isolated noncompaction of ventricular myocardium.

(1 with right NVM and 3 with bilateral NVM), three (3 of 4, 75%) had a dilated RV.

One female patient (1 of 11, 9%) with left NVM had a ventricular aneurysm in the LV apex (Fig. 3). An apical thrombus was found in one adolescent patient (1 of 11, 9%) (Fig. 4), and thrombus of the right brachiocephalic vein and vena cava were subsequently found by other examinations.

DISCUSSION

Noncompaction of ventricular myocardium can co-exist with other congenital cardiac disorders such as an atrial septal defect, interventricular septal defect, pulmonic

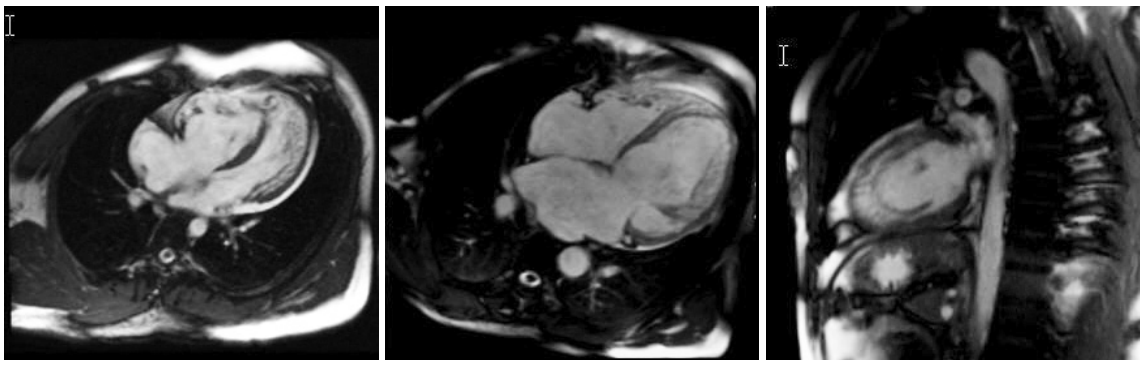

A B C

Fig. 2. Steady-state free precession sequence displaying two-layered structure of ventricular myocardium and high signals within trabecular recesses, suggestive of blood flow communicating with ventricular cavity.

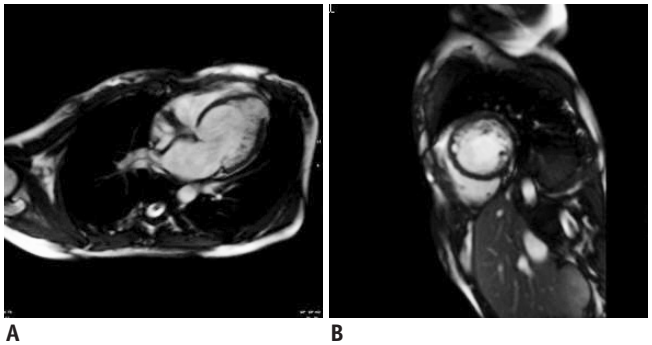

A B

Fig. 3. Steady-state free precession sequence at end of diastolic showing dilated left ventricle and ventricular aneurysm in left ventricular apex (A), septal segment is not affected in short-axis view of left ventricle (B).

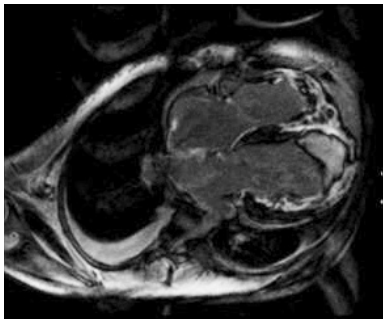

Fig. 4. Apical thrombus (triangle arrow) coexisting with whole heart dilated and delayed enhancement is found in inversion recovery spoiled gradient echo sequence.

stenosis, anomalous pulmonary venous connection, coronary artery anatomical anomalies and Ebstein's syndrome (6-9). In our study, all patients enrolled were isolated NVM and the majority were male. In previous studies, male preponderance has been suggested among adult INVM patients, but no proper evidence has been confirmed (10).

Cardiac MRI is increasingly recognized as an alternative modality for the noninvasive assessment of patients with INVM. Compared with traditional echocardiography, CMRI has less operator dependence, superior spatial resolution, higher contrast between blood and myocardium, which can provide better delineation of the abnormal trabeculations in INVM patients (11). It is particularly useful when the lesions are confined to the ventricular apex, which is difficult to be detected by echocardiography (4, 12). Unfortunately, we were not able to compare echocardiographic and MRI findings, because the affected segments could not be demonstrated in three patients for difficult echocardiographic windows and echocardiographic examination results were not available. Although echocardiographic examination showed hypertrabeculation in the other seven patients, this evidence was not enough to make a specific diagnosis of INVM.

In addition, contrast-enhanced CT is capable of displaying INVM and allow the evaluation of coronary arteries to exclude anomalies or significant stenosis, which is usually not possible with MRI or echocardiography. However, CT remains limited for the detection of myocardial viability, which can be obtained in CMRI by delayed enhancement imaging. To date, there is no consensus about MRI diagnostic criteria for INVM and the main cause of this is the threshold of NC/C ratio. The generally accepted criterion was proposed by Petersen et al. (4) in 2005. They concluded that the ratio of NC/C > 2.3 in the diastole distinguished pathological LV noncompaction with high specificity and sensitivity. Therefore, we used NC/C > 2.3 in diastole as a diagnostic cutoff value to differentiate between normal and pathologic patterns in our series.

Delayed enhancement was seen in six of the nine patients in our study. The patterns of enhancement included subendocardial enhancement and transmural myocardial enhancement. It has been previously reported that delayed enhancement could be found in 70% of INVM

Korean Journal of Radiology
KJR

patients, in both noncompacted compacted segments (3, 5), which was consistent with our findings. Regretfully, the perfusion sequence was not performed in this study. However, hypoperfusion had been previously demonstrated by CMRI and ultrafast CT in NVM patients (13, 14). The histological findings support that delayed enhancement and hypoperfusion are closely related to the abnormalities of the myocardial microcirculation, which result in necrosis, fibrosis, and scar (15-18). Interestingly, the most frequently involved segment was the LV apex, while only one apex had delayed enhancement in our series. This may be due to thinned apical myocardium and the subsequent difficult observation in this area.

In this study, one ventricular aneurysm was observed in LV apex. Few cases of INVM associated with ventricular aneurysm have been reported (5). This may be due to regional ventricular wall thinning (19). Thromboembolic events were observed in one adolescent patient, including thrombus in the LV apex, the right brachiocephalic vein and vena cava. The deep recesses may worsen the risk of thrombus formation and be an additional factor for this serious complication (12).

Four of 11 cases were RV involving INVM in our study (1 right NVM and 3 bilateral NVM). Because it is usually difficult to differentiate pathologic noncompaction from normal trabeculations, the prevalence of RV involvement may have been underestimated in the past. Previously, right INVM has been reported in some cases by CMRI or echocardiography (20). Based on a pathohistologic study, Burke et al. (6) proposed a histological criterion for right NVM: transmural thickness of the noncompacted RV greater than 75%. This criterion was used in our series. It also has been suggested that a diagnosis of right NVM should be made associated with dilatation of the RV (21). In our series, three bilateral INVM had dilated ventricular lumen and only one right INVM had a normal volume. According to the data from our own experience, the dilation of the RV may be a helpful supportive feature for the diagnosis of right NVM.

The clinical manifestation of INVM is highly variable, ranging from no symptoms to a progressive deterioration in cardiac function, arrhythmias, and systemic thromboembolic events. Eight of the 11 patients (73%) in our study had abnormalities in the resting ECG, which were nonspecific, including voltage signs of LV and RV hypertrophy, ST-T segment changes, ventricular premature beat, intraventricular block and pre-excitation syndrome. It has been reported that 94% of adult INVM patients had abnormal ECG manifestations, with ventricular arrhythmias being the most common (12). This may be due to myocardial ischemia and scar tissue induced by microcirculatory dysfunction. Moreover, the prominent trabecular meshwork on the luminal surface of the ventricle was presumed to increase the probability of an ectopic pacemaker and reentrant pathways (12).

The main limitation of our study was that we could not testify the accuracy of > 2.3 as a cutoff value in differentiating pathology myocardium from normal prominent myocardium because of small sample size and retrospective method used in our study. The cases enrolled were not confirmed by the gold standard, which was endomyocardial biopsy. A more comprehensive sequence such as perfusion imaging should be performed in a future study, which may help in the prediction of the prognosis and provide suggestions for treatment.

In conclusion, although the diagnosis of INVM is usually made by echocardiography, CMRI has been increasingly recognized to be particularly useful for assessing the INVM patient. Our findings support the clinical use of CMRI in diagnosing INVM, especially for those patients with suspected diagnoses for an echocardiographic examination. Cine SSFP sequence is a major sequence of CMRI that can represent the contractibility of the myocardium and the ventricular function (22). Characteristic CMRI features of INVM can be clearly revealed in the cine SSFP sequence and black-blood fast SE sequence, which are both important to MRI diagnosis.

REFERENCES

1. Maron BJ, Towbin JA, Thiene G, Antzelevitch C, Corrado D, Arnett D, et al. Contemporary definitions and classification of the cardiomyopathies: an American Heart Association Scientific Statement from the Council on Clinical Cardiology, Heart Failure and Transplantation Committee; Quality of Care and Outcomes Research and Functional Genomics and Translational Biology Interdisciplinary Working Groups; and Council on Epidemiology and Prevention. *Circulation* 2006;113:1807-1816
2. Chin TK, Perloff JK, Williams RG, Jue K, Mohrmann R. Isolated noncompaction of left ventricular myocardium. A study of eight cases. *Circulation* 1990;82:507-513
3. Dursun M, Agayev A, Nisli K, Ertugrul T, Onur I, Oflaz H, et al. MR imaging features of ventricular noncompaction: emphasis on distribution and pattern of fibrosis. *Eur J Radiol* 2010;74:147-151

4. Petersen SE, Selvanayagam JB, Wiesmann F, Robson MD, Francis JM, Anderson RH, et al. Left ventricular non-compaction: insights from cardiovascular magnetic resonance imaging. *J Am Coll Cardiol* 2005;46:101-105
5. Liu X, Kino A, Francois C, Tuite D, Dill K, Carr JC. Cardiac magnetic resonance imaging findings in a patient with noncompaction of ventricular myocardium. *Clin Imaging* 2008;32:223-226
6. Burke A, Mont E, Kutys R, Virmani R. Left ventricular noncompaction: a pathological study of 14 cases. *Hum Pathol* 2005;36:403-411
7. Ichida F. Left ventricular noncompaction. *Circ J* 2009;73:19-26
8. Attenhofer Jost CH, Connolly HM, Warnes CA, O'Leary P, Tajik AJ, Pellikka PA, et al. Noncompacted myocardium in Ebstein's anomaly: initial description in three patients. *J Am Soc Echocardiogr* 2004;17:677-680
9. Betrian Blasco P, Gallardo Agromayor E. Ebstein's anomaly and left ventricular noncompaction association. *Int J Cardiol* 2007;119:264-265
10. Stollberger C, Blazek G, Winkler-Dworak M, Finsterer J. [Sex differences in left ventricular noncompaction in patients with and without neuromuscular disorders]. *Rev Esp Cardiol* 2008;61:130-136
11. Alhabshan F, Smallhorn JF, Golding F, Musewe N, Freedom RM, Yoo SJ. Extent of myocardial non-compaction: comparison between MRI and echocardiographic evaluation. *Pediatr Radiol* 2005;35:1147-1151
12. Oechslin EN, Attenhofer Jost CH, Rojas JR, Kaufmann PA, Jenni R. Long-term follow-up of 34 adults with isolated left ventricular noncompaction: a distinct cardiomyopathy with poor prognosis. *J Am Coll Cardiol* 2000;36:493-500
13. Sato Y, Matsumoto N, Matsuo S, Kunimasa T, Yoda S, Tani S, et al. Myocardial perfusion abnormality and necrosis in a patient with isolated noncompaction of the ventricular myocardium: evaluation by myocardial perfusion SPECT and magnetic resonance imaging. *Int J Cardiol* 2007;120:e24-26
14. Hamamichi Y, Ichida F, Hashimoto I, Uese KH, Miyawaki T, Tsukano S, et al. Isolated noncompaction of the ventricular myocardium: ultrafast computed tomography and magnetic resonance imaging. *Int J Cardiovasc Imaging* 2001;17:305-314
15. Finsterer J, Stollberger C, Feichtinger H. Histological appearance of left ventricular hypertrabeculation/noncompaction. *Cardiology* 2002;98:162-164
16. Junga G, Kneifel S, Von Smekal A, Steinert H, Bauersfeld U. Myocardial ischaemia in children with isolated ventricular non-compaction. *Eur Heart J* 1999;20:910-916
17. Jenni R, Wyss CA, Oechslin EN, Kaufmann PA. Isolated ventricular noncompaction is associated with coronary microcirculatory dysfunction. *J Am Coll Cardiol* 2002;39:450-454
18. Jassal DS, Nomura CH, Neilan TG, Holmvang G, Fatima U, Januzzi J, et al. Delayed enhancement cardiac MR imaging in noncompaction of left ventricular myocardium. *J Cardiovasc Magn Reson* 2006;8:489-491
19. Sato Y, Matsumoto N, Yoda S, Inoue F, Kunimoto S, Fukamizu S, et al. Left ventricular aneurysm associated with isolated noncompaction of the ventricular myocardium. *Heart Vessels* 2006;21:192-194
20. Sato Y, Matsumoto N, Matsuo S, Sakai Y, Kunimasa T, Imai S, et al. Right ventricular involvement in a patient with isolated noncompaction of the ventricular myocardium. *Cardiovasc Revasc Med* 2007;8:275-277
21. Fazio G, Lunetta M, Grassedonio E, Gullotti A, Ferro G, Bacarella D, et al. Noncompaction of the right ventricle. *Pediatr Cardiol* 2010;31:576-578
22. Kim KA, Seo JB, Do KH, Heo JN, Lee YK, Song JW, et al. Differentiation of recently infarcted myocardium from chronic myocardial scar: the value of contrast-enhanced SSFP-based cine MR imaging. *Korean J Radiol* 2006;7:14-19